



Coronary stent CD31-mimetic coating favours endothelialization and reduces local inflammation and neointimal development *in vivo*

Sergio Diaz-Rodriguez^{1†}, Charlotte Rasser^{2†}, Jules Mesnier², Pascale Chevallier¹, Romain Gallet³, Christine Choqueux², Guillaume Even², Neila Sayah², Frédéric Chaubet², Antonino Nicoletti², Bijan Ghaleh³, Laurent J Feldman^{2,4}, Diego Mantovani¹, and Giuseppina Caligiuri^{2,4*}

¹Laboratory for Biomaterials and Bioengineering (CRC-I) Department of Min-Met-Mat Engineering and the CHU de Québec Research Center, Laval University, PLT-1745G, Québec, QC G1V 0A6, Canada; ²Laboratory for Vascular Translational Science, Université de Paris, Inserm U1148, 46 rue Henri HUCHARD, Paris 75018, France; ³Institut Mondor de Recherche Biomédicale, école nationale vétérinaire de Maisons-Alfort (ENVA), Institut National de la Santé et de la Recherche Médicale U955, GHU (Groupe Hospitalo-Universitaire) A. Chenevier, Henri Mondor Faculty of Medicine Paris Est, 8 Rue du Général Sarraill, Créteil 94010, France; and ⁴Department of Cardiology, Assistance Publique-Hôpitaux de Paris, Hôpitaux Universitaires Paris Nord Val-de-Seine, Site Bichat, 46 rue Henri Huchard, Paris 75018, France

Received 29 April 2020; revised 12 October 2020; editorial decision 12 January 2021; accepted 12 January 2021; online publish-ahead-of-print 13 February 2021

See page 1770 for the editorial comment on this article (doi: 10.1093/eurheartj/ehab091)

Aims

The rapid endothelialization of bare metal stents (BMS) is counterbalanced by inflammation-induced neointimal growth. Drug-eluting stents (DES) prevent leukocyte activation but impair endothelialization, delaying effective device integration into arterial walls. Previously, we have shown that engaging the vascular CD31 co-receptor is crucial for endothelial and leukocyte homeostasis and arterial healing. Furthermore, we have shown that a soluble synthetic peptide (known as P8RI) acts like a CD31 agonist. The aim of this study was to evaluate the effect of CD31-mimetic metal stent coating on the *in vitro* adherence of endothelial cells (ECs) and blood elements and the *in vivo* strut coverage and neointimal growth.

Methods and results

We produced Cobalt Chromium discs and stents coated with a CD31-mimetic peptide through two procedures, plasma amination or dip-coating, both yielding comparable results. We found that CD31-mimetic discs significantly reduced the extent of primary human coronary artery EC and blood platelet/leukocyte activation *in vitro*. *In vivo*, CD31-mimetic stent properties were compared with those of DES and BMS by coronarography and microscopy at 7 and 28 days post-implantation in pig coronary arteries ($n=9$ stents/group/timepoint). Seven days post-implantation, only CD31-mimetic struts were fully endothelialized with no activated platelets/leukocytes. At day 28, neointima development over CD31-mimetic stents was significantly reduced compared to BMS, appearing as a normal arterial media with the absence of thrombosis contrary to DES.

Conclusion

CD31-mimetic coating favours vascular homeostasis and arterial wall healing, preventing in-stent stenosis and thrombosis. Hence, such coatings seem to improve the metal stent biocompatibility.

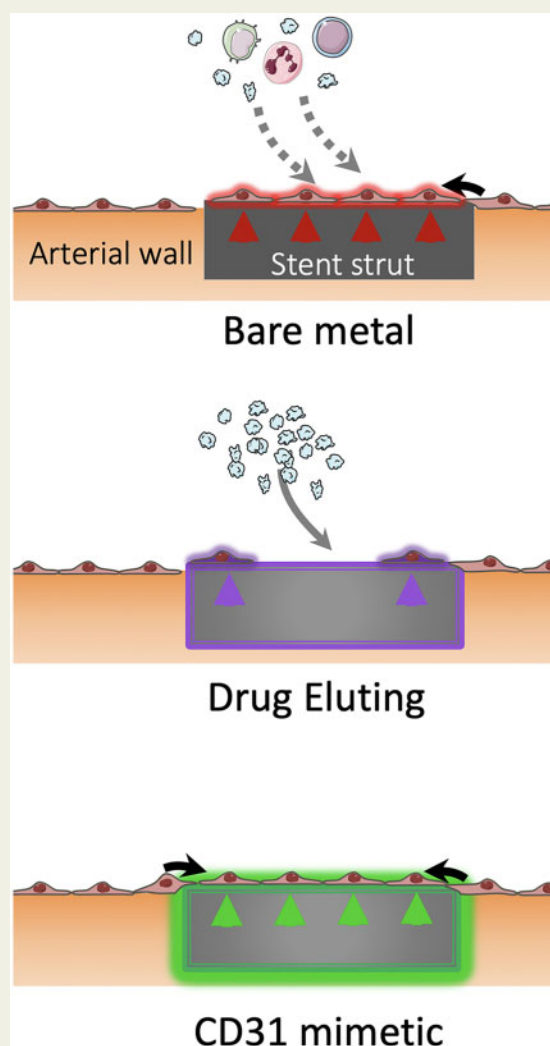
* Corresponding author. Tel: +33 1 40 25 75 56, Fax: +33 1 40 25 86 02, Email: giuseppina.caligiuri@inserm.fr

† These authors are co-first authors.

© The Author(s) 2021. Published by Oxford University Press on behalf of the European Society of Cardiology.

This is an Open Access article distributed under the terms of the Creative Commons Attribution Non-Commercial License (<http://creativecommons.org/licenses/by-nc/4.0/>), which permits non-commercial re-use, distribution, and reproduction in any medium, provided the original work is properly cited. For commercial re-use, please contact journals.permissions@oup.com

Graphical Abstract



CD31 mimetic coating favours the growth of a physiologic endothelial wall on stent struts: bare metal, drug-eluting and CD31-mimetic.

Keywords

Coronary • Stent • Biocompatibility • CD31 • Biomimetic device • Endothelium

Translational perspective

The CD31-mimetic stent might constitute a promising biocompatible pro-healing, anti-inflammatory, anti-thrombotic metal stent for the treatment of coronary disease, while preventing neointimal development and in-stent stenosis. The use of CD31-mimetic stents could become a supportive interventional coronary treatment on the medium-long term.

Introduction

The aim of endovascular stent implantation at the time of coronary angioplasty is to prevent acute vessel closure and chronic negative arterial remodelling in patients affected by coronary disease. However, stents are sensed as a foreign body leading to immune cell activation,¹ resulting in chronic inflammation and eventually in-stent restenosis due to the local proliferation of arterial smooth muscle cells.²

Mitigating the body reaction by improving stent biocompatibility thus represents a main challenge to increase the efficacy of arterial stents and hence the clinical outcome of patients affected by coronary disease.

Drug-eluting stents (DES), embedded in a polymer allowing local release of anti-inflammatory/anti-proliferative drugs,^{3,4} were developed to avoid such secondary effects. However, despite the routine use of prolonged dual antiplatelet therapy, stent-associated

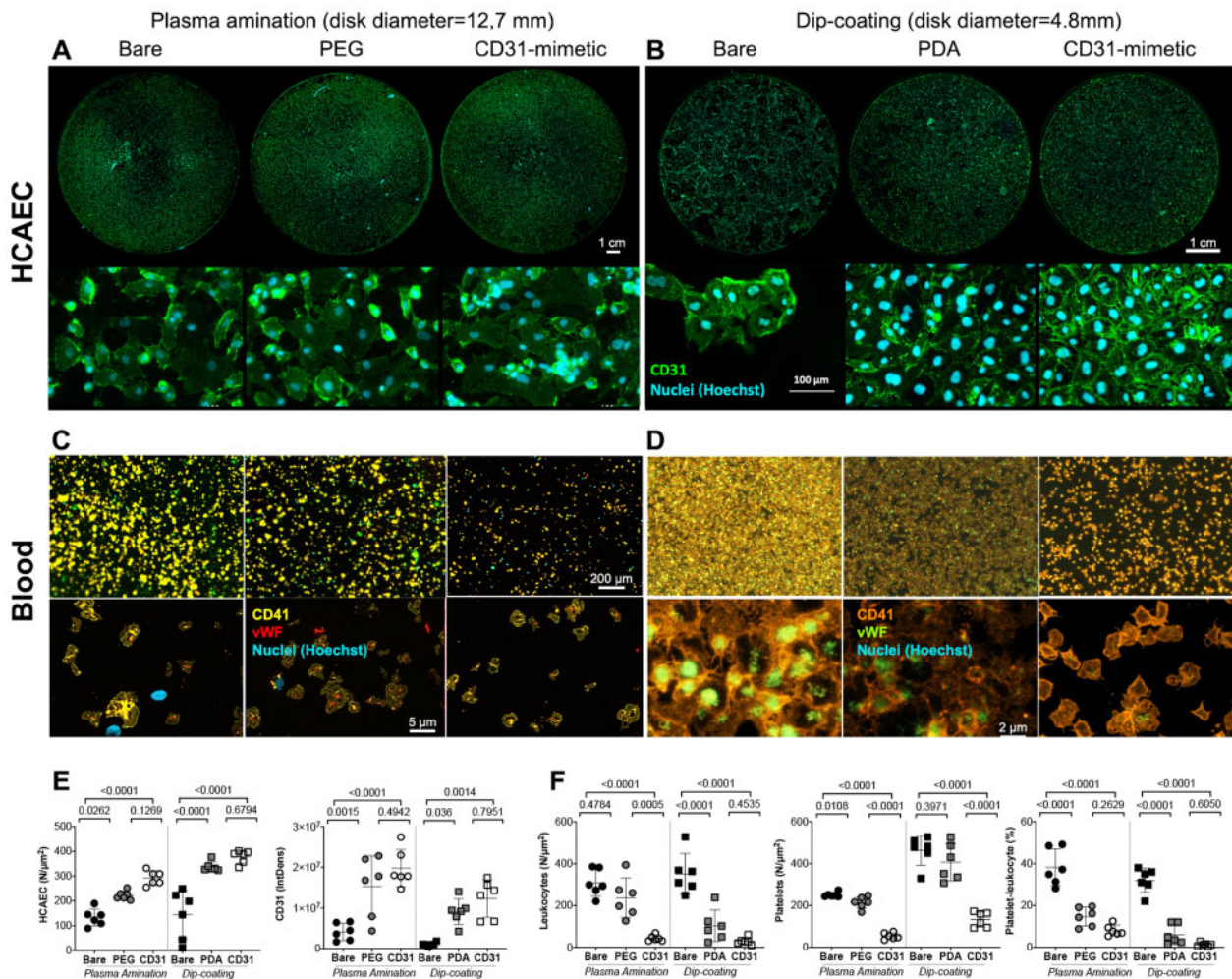


Figure 1 *In vitro* analysis of human coronary artery endothelial cells and blood elements adhering to CD31-mimetic Cobalt Chromium discs. (A–D) Representative digital fluorescent images of human coronary artery endothelial cells and human blood elements interacting with Cobalt Chromium discs obtained by either plasma amination (A, C) or dip-coating (B, D) procedures. Controls for plasma amination included discs subjected to electro-polishing alone (bare) or completed with poly(ethylene glycol) bis(carboxymethyl) ether linker covalent binding. Control discs for dip-coating were subjected to ultrasound cleaning in acidic water (bare) or completed with the self-assembly of a thin polydopamine film. (E) Human coronary artery endothelial cells adhering on the experimental discs were quantified in terms of number/surface (count of nuclei, i.e. Hoechst staining, expressed as $N/\mu\text{m}^2$) and of integrated density of CD31 at the cell–cell border (green, IntDens, arbitrary units). Both parameters were significantly greater in coated as compared to bare metal discs; the presence of the CD31 peptide tended to yield higher values compared to poly(ethylene glycol) bis(carboxymethyl) ether or polydopamine coatings, although the difference did not reach statistical significance. (F) Blood leukocytes and platelets were quantified individually ($N/\mu\text{m}^2$) by analysing the fluorescent particles in the blue (nuclei = leukocytes, Hoechst+ particles) and orange (platelets = CD41^+ particles) channels, respectively, and as aggregates (% of total elements) by counting the number of blue elements overlapping orange elements. von Willebrand factor+ immune staining within platelets (red in the left panel and green in the right panel) was also analysed. Of note, the number of von Willebrand factor+ elements yielded identical data as for the CD41^+ element analysis (data not shown). Polydopamine and poly(ethylene glycol) bis(carboxymethyl) ether coatings were able to reduce blood leukocyte adherence and platelet-leukocyte aggregates (especially polydopamine) but, importantly, both failed to reduce platelet adherence and the latter was reduced only in the presence of the CD31 peptide. The indicated scale bars apply to all the images of the same row.

thrombosis may occur late after DES implantation due to prothrombotic and/or hypersensitivity reactions triggered by the polymer and/or the drugs.^{5,6} Moreover, lower rates of stent endothelialization have been reported.⁷

An alternative strategy to the local delivery of immune suppressive drugs could be to prevent the inflammatory reaction with a stent

perceived as 'self' by adjacent endothelial cells (ECs), circulating platelets, and leukocytes. In this regard, CD31 might be a compelling target. Indeed, this constitutive co-receptor also known as platelet EC adhesion molecule 1 is expressed at the surface of blood platelets and leukocytes and is the most abundant protein at the EC surface and exerts key regulatory functions for circulation homeostasis by

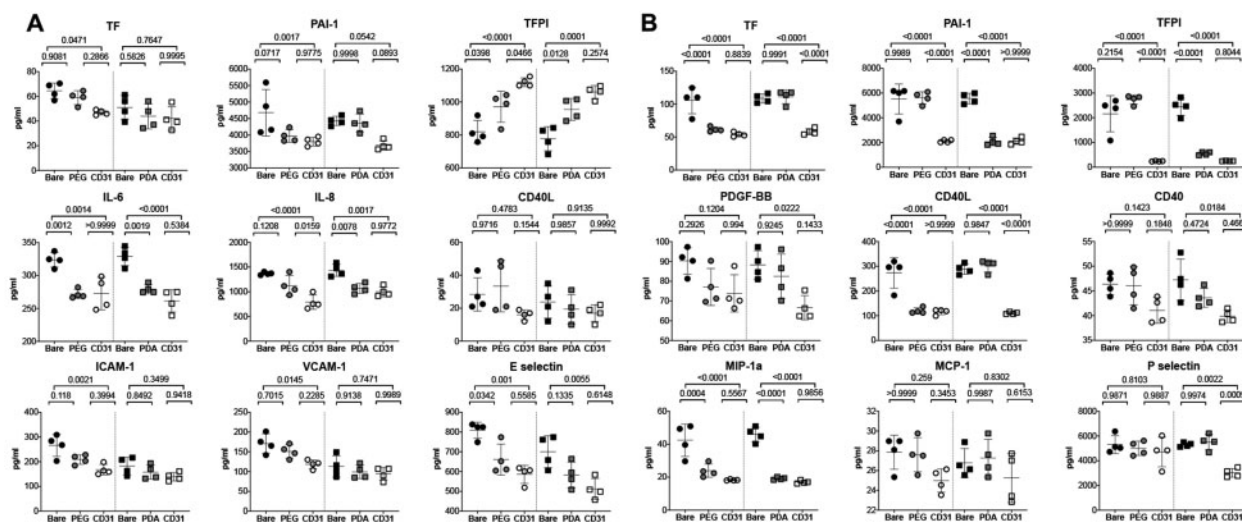


Figure 2 *In vitro* analysis of soluble markers released by human coronary artery endothelial cells and blood elements in contact with CD31-mimetic Cobalt Chromium discs. (A and B) Quantitative analysis of coagulation and inflammation soluble factors released in the supernatant of human coronary artery endothelial cells cultured during 48 h (A) or released in the blood-derived plasma after 1 h of incubation under continuous rotation (B), in the presence of CD31-mimetic Cobalt Chromium-coated discs or their controls. Individual points are median values from eight replicates of four different donors. The release of plasminogen activator-1, interleukin-6, interleukin-8, E-selectin in the supernatant of human coronary artery endothelial cells and the secretion of tissue factor, plasminogen activator-1, tissue factor pathway inhibitor, CD40L, macrophage inflammatory protein-1 alpha in the plasma derived from the blood incubated with the experimental discs was significantly reduced by the presence of the CD31 peptide, regardless of the type of linker arm used [i.e. poly(ethylene glycol) bis(carboxymethyl) ether or polydopamine]. Furthermore, human coronary artery endothelial cell release of soluble tissue factor pathway inhibitor was significantly increased in the presence of the CD31-mimetic peptide compared to bare and poly(ethylene glycol) bis(carboxymethyl) ether controls, reflecting a CD31-dependent physiologic anticoagulant function of the endothelium. ICAM-1, intercellular adhesion molecule-1; PDGF-BB, platelet-derived growth factor-BB; VCAM-1, vascular cell adhesion molecule 1. Circles: plasma amination; squares: dip-coating.

co-clustering with key membrane signalling receptors, upon intercellular *trans*-homophilic binding (reviewed in⁸). Importantly, we have shown that a soluble synthetic peptide (P8RI), binding to the juxta-membrane CD31 extracellular sequence involved in the receptor clustering, acts like a CD31 agonist (reviewed in⁹). Here, we asked whether immobilizing P8RI onto metal stents could reduce the reaction of vascular and blood cells forging contact with the device. To do so, we studied the potential clinical application of CD31-mimetic coatings with P8RI. First, we characterized the *in vitro* blood platelet/leucocyte reaction and phenotype of ECs growing onto CD31-mimetic coated discs. Second, we evaluated the *in vivo* effects on the blood and vascular response to whole CD31-mimetic stents implanted in pig coronary arteries.

Methods

Surface functionalization and peptide grafting

Plasma amination

Cobalt Chromium (CoCr) flat discs (12.7-mm diameter, 0.15-mm thick, cut out of L-605 sheets from Rolled Alloys Inc., Laval, QC, Canada) were subjected to electropolishing and plasma amination through a two-step process using a mixture of N₂ and H₂, as detailed in.¹⁰ Resulting reactive

amine groups present at the alloy surface were used as anchor points for the grafting of the CD31-mimetic peptide (P8RI, sequence H-kwpalfvr-OH, described in detail in¹¹) via a poly(ethylene glycol) bis(carboxymethyl) ether (PEG)-linking arm and carbodiimide chemistry, as described.¹⁰

Dip-coating

CoCr flat discs (4.8-mm diameter, 0.15-mm thick) were provided as mirror polished by a controlled industrial workshop (Goodfellow Cambridge Ltd, Huntingdon, UK). CoCr discs and unmounted stents were ultrasound cleaned in successive acidic, alcoholic, and water baths. Functionalization was achieved by the deposition of a self-assembled biopolymer [polydopamine (PDA)], as described.^{12,13} Two successive dip-coating steps in solutions containing a flexible linker (BCN-amine, Sigma Aldrich) and an N-terminal azide P8RI (N3-kwpalfvr-OH, synthesized by ProteoGenix Inc., Schiltigheim, France) allowed for a copper-free click-chemistry biorthogonal immobilization as described.¹⁴ Coating uniformity was confirmed by fluorescence microscopy and its persistence evaluated by X-ray photoelectron spectroscopy survey analyses after passage in an accelerated ageing bench test¹⁵ (Supplementary material online).

Multilink[®] commercial stents were deployed, unmounted from their catheter, and subjected to CD31 peptide grafting by both plasma amination and dip-coating. Coated stents were cramped back onto the catheter using tweezers and sterilized by beta radiations (25 kGy) prior to *in vivo* use.

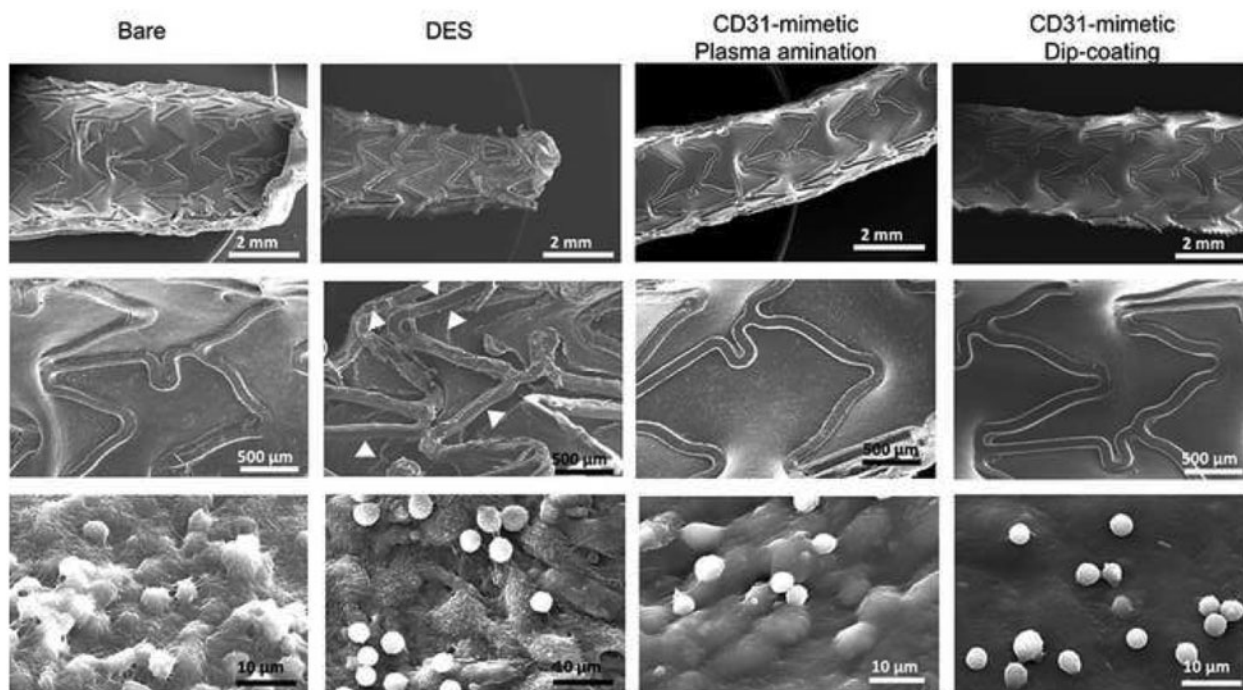


Figure 3 *In vivo* stent endothelialization at day 7 post-implantation. Representative examples of scanning electron microscopy imaging of the luminal surface of pig coronary arteries implanted with either bare metal or drug-eluting stent vs. CD31-mimetic plasma aminated or dip-coated stents ($n = 9$ stents/group), taken at low (top), medium (middle) or high (bottom) magnification. Arrowheads point at the absence of endothelialization over the drug-eluting stent struts. Note the presence of activated leukocytes (numerous pseudopods at their surface) tangled in a dense fibrin mesh over the endothelialized struts of bare metal stents. Non-activated (round-shaped) leukocytes can be identified over drug-eluting stent struts but there endothelial cells appeared detached one from another and covered with platelets and fibrin. Instead, the absence of leukocyte activation (round shape) was combined with the presence of a smooth and continuous endothelium, free from platelets and fibrin, over CD31-mimetic stent struts.

Analysis of CD31-mimetic Cobalt Chromium disc biocompatibility

Electropolished discs +/- the PEG linker served as controls for the plasma amination coating procedure whereas ultrasound cleansed and PDA-BCN linker discs were used for comparison with dip-coated CD31-mimetic discs.

Human primary coronary artery ECs (HCAECs from four donors, Lonza) were seeded at high density ($1 \times 10^5/\text{cm}^2$) onto CD31-mimetic CoCr discs and cultured in EC basal medium for 48 h (beyond 48 h, HCAECs likely began to decay in the absence of endothelial growth factors). Cells adhering onto the experimental discs were stained with anti-human CD31 antibodies (mouse clone JC70/A, DAKO and Alexafluor[®] 488 goat anti-mouse IgG; Jackson ImmunoResearch) and Hoechst 33342 (nuclei). Soluble tissue factor (TF), plasminogen activator inhibitor 1 (PAI-1), TF pathway inhibitor (TFPI), interleukin (IL)-6, IL-8, CD40L, intercellular adhesion molecule 1, vascular cell adhesion molecule 1, and E-selectin were analysed in culture supernatants on a BioPlex200[®] analyser (Bio-Rad).

Human whole blood collected in PPack (CryoPep, Montpellier, France) was deposited onto the discs in 96-well plates incubated on an orbital shaker (medium speed) at 37°C for 1 or 24 h. Individual plasma samples were used for measuring plasma soluble TF, PAI-1, TFPI, platelet-derived growth factor-BB, CD40L, CD40, macrophage inflammatory protein-1 (MIP-1), monocyte chemoattractant protein-1 and P-selectin

(BioPlex200[®], Bio-Rad) and the discs were processed for fluorescence microscopy. Anti-human CD41 (mouse clone P2, Beckman Coulter) and anti-von Willebrand factor (rabbit polyclonal, DAKO) primary antibodies and rhodamine or AlexaFluor[®] 488-conjugated secondary antibodies (from Jackson ImmunoResearch) served to identify platelets whereas the nuclei (Hoechst 33342 staining) identified the leukocytes.

Experimental discs with fluorescently labelled adherent elements were mounted face-down on ibidi[®] imaging μ -dishes, imaged with an Axio Observer microscope equipped with the Zen software (Zeiss), and analysed with the 'Analyze Particles' command of Image J[®] (NIH). Adherent elements were counted (N/mm^2) and positive staining quantified as integrated density (IntDens).

In vivo evaluation of CD31-mimetic stents

Coronary stent implantation in female farm pigs was performed as described in the [Supplementary material online](#). All four stent types [everolimus-eluting, durable polymer-coated Xience[®] stents, DES group; polymer-free, unmodified Multilink[®] BMS, bare metal stent (BMS) group (both kindly provided by Abbott Vascular); or CD31-mimetic stents (plasma aminated or dip-coated)] were implanted in the three coronary arteries (one type of stent per animal) in a total of 24 female farm pigs. Aspirin (75 mg/day) and ticagrelor (90 mg bid) were continued orally until termination (by vecuronium overdose followed by perfusion with a saturated KCl solution, under general anaesthesia). A total of nine stents per

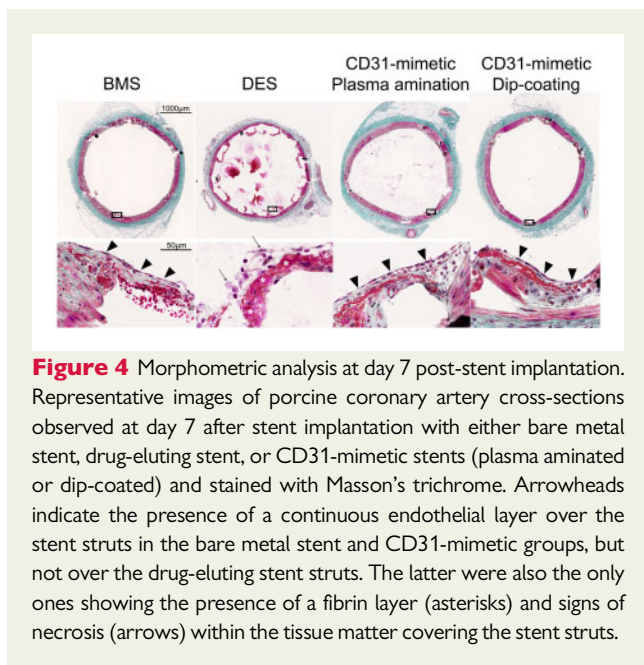


Figure 4 Morphometric analysis at day 7 post-stent implantation. Representative images of porcine coronary artery cross-sections observed at day 7 after stent implantation with either bare metal stent, drug-eluting stent, or CD31-mimetic stents (plasma aminated or dip-coated) and stained with Masson's trichrome. Arrowheads indicate the presence of a continuous endothelial layer over the stent struts in the bare metal stent and CD31-mimetic groups, but not over the drug-eluting stent struts. The latter were also the only ones showing the presence of a fibrin layer (asterisks) and signs of necrosis (arrows) within the tissue matter covering the stent struts.

group (one in each of the three coronary arteries, $n = 3$ pigs for each group) were implanted for each timepoint (12 pigs per timepoint). Coronary angiography was repeated on study termination day. Stented arteries were explanted, rinsed in phosphate buffered saline (PBS), and fixed in formaldehyde for 48 h prior to final processing.

Coronary angiography and stent explantation were performed at 7 days after stenting (three pigs/group) for the analysis of endothelialization by scanning electron microscopy as previously described¹⁶ and histomorphometry analysis of Masson's trichrome-stained sections.

Stenosis was evaluated at 28 days (three pigs/group) by coronary angiography and histomorphometry by Masson's trichrome-stained resin cross-sections. Computer-assisted image analysis served to calculate the lumen surface area reduction by the neointima on three cross-sections (proximal, medial, and distal) from each stented artery ($n = 9$ /stent group) using the QWin[®] software (Leica) on Sirius Red-stained sections imaged under fluorescence, as previously described.¹⁷

Statistical analysis

Data are presented as individual points. One-way ANOVA and Tukey's multiple comparison test with Prism[®] 8 were used to compare individual groups. Adjusted P -values are reported next to all graphs in the figures.

Results

Analyses of blood and arterial endothelial cells interacting with CD31-mimetic coated Cobalt Chromium surfaces

None of the experimental discs caused significant haemolysis at 1 or 24 h (Supplementary material online). The number of adherent HCAECs and the extent of CD31⁺ lateral junctions were significantly increased when the cells grew onto CD31-mimetic discs,

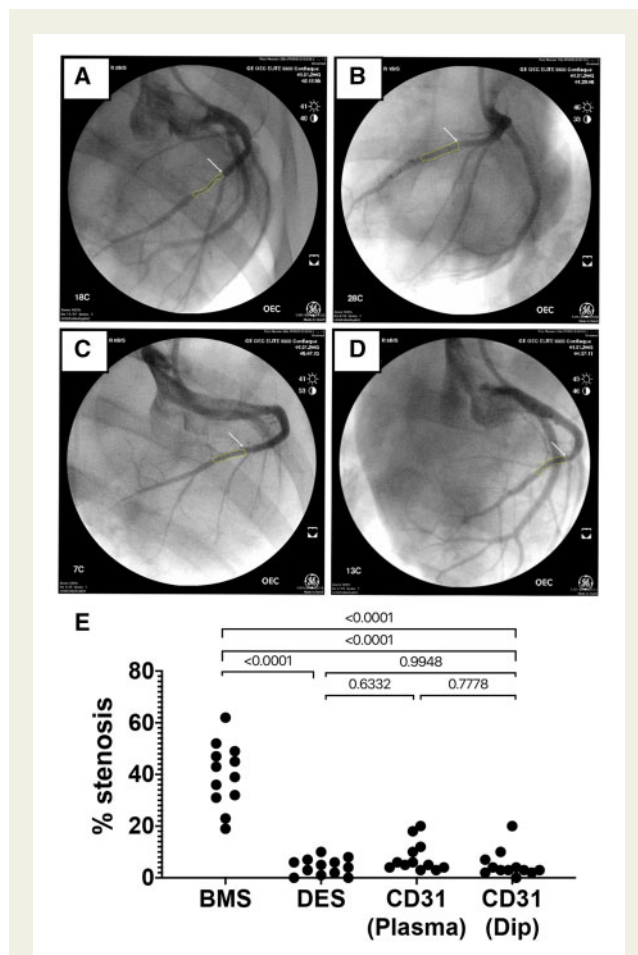


Figure 5 Evaluation of in-stent stenosis by coronary angiography at day 28. Representative angiography images of the left coronary arteries at 28 days after implantation of either bare metal stent (A), drug-eluting stent (B), plasma aminated (C), or dip-coated (D) CD31-mimetic stents. White arrows: proximal edge of the implanted stent. Yellow outlines: lumen shape within the stent. (E) Quantitative analysis of coronary stenosis (% lumen size reduction). The extent of stenosis was comparable in drug-eluting stent and CD31-mimetic stent groups and significantly lower compared to the bare metal stent group, regardless of the coronary artery type.

compared to bare controls (Figure 1). A moderate increase was also observed with bioactive PEG- and PDA-coated discs as compared to bare samples. Importantly, CD31-mimetic coating significantly reduced leucocyte and platelet adhesion to the experimental discs (see plasma amination condition), while platelet adhesion was unchanged with PDA and PEG alone coatings and only PDA coating reduced the extent of blood leucocyte adhesion (Figure 1). The addition of the CD31 peptide tended, more than PEG and PDA alone, to reduce the frequency of platelet-leucocyte aggregates observed on PEG or PDA functionalized as compared to bare surfaces (Figure 1).

Quantitative analysis of coagulation and inflammation soluble biomarkers, using the supernatant of HCAECs and of human blood

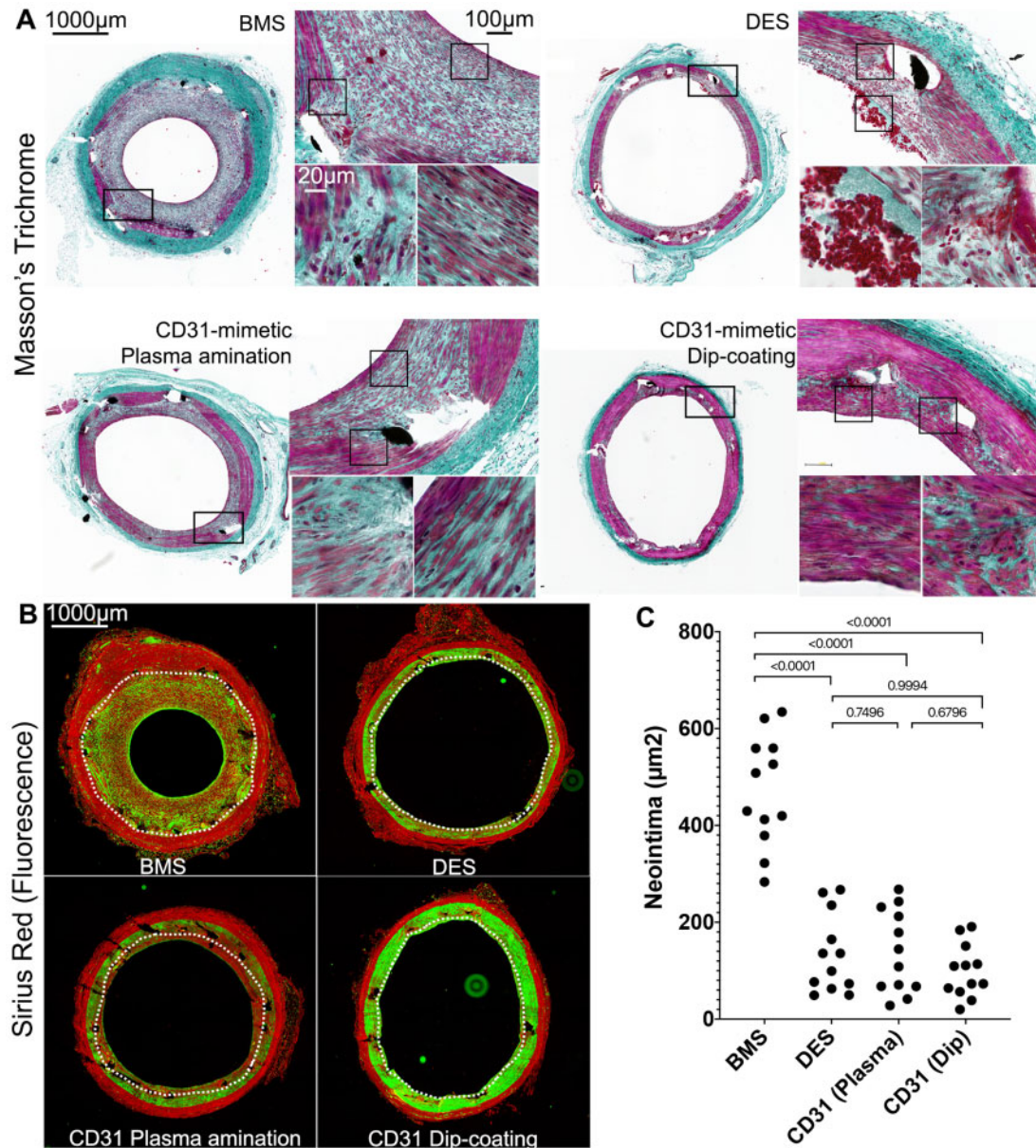


Figure 6 Morphometric analysis of the neointima at day 28. Composition of in-stent neointima at 28 days after stent implantation. (A) Masson's trichrome staining. Black = nuclei, deep green = extracellular matrix, purple = cell cytoplasm, red = erythrocytes; light green/grey = ancient fibrin/platelets. Note the thick neointima and presence of leukocytes (black round nuclei) with the bare metal stent, the presence of fibrin, platelets, and erythrocytes with the drug-eluting stent and the organized media-like structure of the thin neointima with the CD31-mimetic stents. The black squares in low magnification images indicate the localization of the magnified insets. (B) Fluorescence microscopy analysis of Sirius Red-stained resin cross-sections of stented arteries. Red = collagen and elastin; green = stromal cell cytoplasm. White dotted line = internal elastic lamina. Note the consistent presence of stromal cells (green) in the media of arteries implanted with CD31-mimetic stents as compared to their paucity when implanted with drug-eluting stent and virtual absence with bare metal stent. Several stromal cells were also visible with bare metal stent but localized in the neointima (tissue growing inward of the stent struts and internal elastic lamina). (C) Quantitative analysis of neointima surface area (μm^2). Individual points are median values from three sections (proximal, middle and distal cross-section) of each sample.

from individual culture wells containing the experimental discs, supported the above observations (Figure 2). Whereas coating with PEG or PDA alone was able to blunt most inflammatory markers, CD31-mimetic coating consistently reduced the release of both pro-inflammatory and pro-coagulant molecules secreted by adherent ECs or blood elements, independently of the coating procedure and of the respective intermediate functional layer. In particular, CD31-mimetic coating reduced the levels of TF and PAI-1 and increased, in a mirror fashion, the levels of TFPI (Figure 2), an effect particularly evident with the plasma amination procedure, reflecting a CD31-specific HCAEC anticoagulant phenotype.

Effect of CD31-mimetic stents on *in vivo* strut endothelialization

Control coronary angiography at day 7 showed no detectable lumen size modification in any group (Supplementary material online). Scanning electron microscopy of the luminal side of stented arteries revealed complete stent strut endothelialization in both BMS and CD31-mimetic stents (Figure 3). In contrast, a patchy, discontinuous layer of ECs was visible on DES, consistent with previous reports.¹⁸ A few, round-shaped (non-activated), blood leukocytes were observed in DES and CD31-mimetic stents. In contrast, the leukocytes attached to the endothelium covering the BMS showed multiple interconnected pseudopods and shape asymmetry, typical of recent activation (Figure 3). Morphometric analysis on cross-sections confirmed the presence of a continuous endothelial layer covering the struts of both BMS and CD31-mimetic stents at day 7, whereas an unstructured tissue, made of fibrin and dying cells (comprising arterial cells and leukocytes), covered DES struts (Figure 4).

Effect of CD31-mimetic stents on in-stent stenosis

Luminal size reduction (stenosis, expressed as % of the lumen size traced on native lumen contrast images) was analysed in each of the three stented coronary arteries from all remaining 12 pigs, 28 days after stent implantation ($n = 3$ pigs/stent group). The degree of stenosis in each of the three implanted coronary arteries was consistently greater in BMS compared to CD31-mimetic stents and DES (Figure 5). The angiographic data were confirmed by histomorphometry analyses on resin cross-sections (Figure 6). Fluorescent images of Sirius Red-stained sections, allowing automatic detection of the internal elastic lamina in the red channel, were used to quantify the extent of stenosis (Figure 6). BMS stent cross-sections consistently showed lumen stenosis and the presence of fibrosis (collagen content in the neointima + media). In comparison, the extent of neointima and fibrosis were significantly lower in DES and CD31-mimetic stents, obtained by either plasma amination or dip-coating (Figure 6 and Supplementary material online). Of note, at variance with DES, the structure of the thin neointima in the stented arteries in CD31-mimetic groups resembled a normal arterial media, composed of parallel layers of smooth muscle cells in between elastin/collagen sheets (Figure 6). Remarkably, in spite of the dual antiplatelet treatment with aspirin and ticagrelor at full doses, DES-implanted arteries (but not BMS and CD31-mimetic stents) showed signs of local thrombosis (Figure 6).

Discussion

In our *in vitro* assays, we show that CD31-mimetic coatings (i) reduce leucocyte and platelet adherence/activation/aggregation, (ii) improve metal surface endothelialization, and (iii) maintain a HCAEC physiological phenotype (low release of soluble inflammatory/thrombotic biomarkers), as compared to bare metal devices. Importantly, only CD31 coatings achieved the combination of all these effects, as compared to bare and PEG- and PDA-coated devices. However, as expected from previous bioengineering studies, the linkers PEG and PDA also conferred a certain degree of biocompatibility to CoCr surfaces as observed in our *in vitro* experiments.^{19,20} Nonetheless, contrary to HCAECs growing onto CD31-mimetic surfaces, HCAECs growing onto PEG and PDA coatings released several soluble inflammatory/thrombotic biomarkers. Furthermore, PDA and PEG surfaces had no or only a minor effect, respectively, on reducing blood platelet adhesion. Hence, PDA and PEG coatings alone would presumably not reduce the risk of thrombosis inherent to metal devices, contrary to what our results strongly suggest with CD31-mimetic stents. Consistent with our previous work demonstrating that soluble P8RI drives cell-specific outside-in co-signalling guaranteeing vascular homeostasis, we believe that CD31-coating, on top of PEG or PDA linkers, acts through specific engagement of cell surface CD31 in different vascular cell types. Indeed, CD31-coating presumably stabilizes resident EC adherence while driving a detachment signal in circulating blood cells (recently reviewed in⁹).

These homeostatic properties were confirmed in our *in vivo* study. Indeed, we further report that the CD31-mimetic coating promotes *in vivo* vascular wall healing while reducing the adverse reactions leading to in-stent stenosis and thrombosis in comparison to BMS and DES, respectively. While fast endothelialization occurs in the presence of BMS, endothelium and circulating cell reactivity towards the foreignness of metal devices eventually leads to in-stent stenosis. Our study indicates that the CD31-mimetic coating is efficient both for rapid endothelialization and to 'hide' the foreign metal material from reactive blood solid and soluble reactive elements. This leads to the formation of a seemingly physiologic endothelial barrier, with anti-inflammatory and anti-thrombotic properties. Indeed, we observed that the neointima formed at day 28 post-implantation with the CD31-mimetic stents was as thin as in DES and significantly thinner than in BMS. In particular, the structure of the tissue covering CD31-mimetic struts was composed of organized layers of extracellular matrix alternated with elongated mesenchymal cells (likely smooth muscle), presumably endowing the stented segment with recovered contractile and elastic arterial wall properties, at variance with the tissue surrounding the BMS, which was highly fibrotic.

Importantly, as mentioned, the effect of CD31-mimetic stents is most likely inherent to the CD31-dependent homeostatic regulation⁸ elicited by the direct contact of vascular cells with the stent surface and does not require the release of a bioactive compound. Thus, the CD31 coating prevents the adverse reaction of vascular and blood cells while the metal surface is exposed. Thereafter, once a complete and functional endothelium has completely hidden the device, the exposure to the peptide is presumably no longer required as the luminal surface with the stented segment strikingly resembles that of the adjacent normal artery and should thus continue to behave physiologically on the long term. We therefore believe that our

CD31-mimetic coating could meet the improvement expected in the stent field (reviewed in²⁰). Of note, the time points for endothelialization and stenosis assessment were based on previous reports and the consensus reached by the experts in the preclinical stent evaluation field (reviewed in¹⁹). Although beyond the scope of our work, a later timepoint (at 120 days) would be necessary in the translational perspective. Furthermore, future studies validating the efficacy of CD31-mimetic coating should be carried out in atheromatous conditions.

Remarkably, the anti-stenotic effect of DES was counterbalanced by incomplete endothelialization at day 7 and presence of luminal clots at day 28 despite continued dual antiplatelet treatment, consistent with previous findings.¹⁶ Indeed, the antimitotic effect of the drugs released by the DES also acts on ECs,¹⁸ inhibiting endothelialization. Instead, the anti-inflammatory effect of CD31 coating was consistently accompanied by an anti-thrombotic effect. If confirmed in future studies, the CD31-mimetic coating could lead to a lightened use of antiplatelet drugs, which would further increase the clinical interest for the development of CD31-mimetic stents.

Although the plasma functionalization approach had served as proof of concept in previous studies,¹⁰ this procedure cannot easily be scaled up by industrial manufacturers. Furthermore, plasma treatment cannot be applied to any substrate as electropolishing can affect the uniformity of deposited films on certain surfaces such as nitinol, hence, the dip-coating procedure development involving PDA. Indeed, this coating method is robust, straightforward and, as mentioned above, our results strongly suggest that the presence of PDA as a linker arm does not hinder or alter the P8RI-dependent CD31-mimetic effect. Thus, the dip-coating procedure is well-suited for scaling-up and manufacturing practice. Future clinical trials could soon confirm this potential.

Other coating strategies aiming at favouring stent endothelialization have recently emerged. The Genous[®] stent, functionalized with anti-CD34 antibodies, was intended to capture circulating CD34⁺ endothelial progenitor cells,²¹ but it showed a higher risk of restenosis compared to DES.^{22–24} The addition of an abluminal bioabsorbable polymer-eluting sirolimus (Combo[®] stent)^{25,26} reverted the restenosis risk, but the endothelial coverage is actually lower than with DES.²⁷ This is presumably due to the low frequency of circulating progenitor ECs (0.2% of nucleated blood elements) in coronary patients.²⁸ Another approach uses short peptide sequences mimicking the presence of extracellular matrix to favour the attachment of adjacent ECs via their integrins. Preliminary experimental studies with a cyclic-RGD (Arg-Gly-Asp) peptide-coated stent showed interesting pro-endothelial properties *in vivo*,²⁹ but possible engagement of integrins on blood³⁰ and smooth muscle cells³¹ may bring back the risk of thrombosis and restenosis. Instead, CD31-mimetic stents selectively favour the adhesion of ECs, not of smooth muscle cells or blood elements.

In conclusion, our results suggest that CD31-mimetic coating both favours CoCr stent integration while promoting arterial wall healing around stent struts. To our knowledge, this would be the first stent, which likely uses endogenous homeostasis regulation common to all vascular cells, both circulating and resident, hence its potential pleiotropic effects on arterial wall healing.

Supplementary material

Supplementary material is available at *European Heart Journal* online.

Acknowledgements

We are indebted to Armelle Babonneau, Gérard Partouche, Lucien Sambin, and Alain Bizé for their precious help with the organization of the *in vivo* experiments and to Melanie Gettings for critical reading and help with manuscript editing.

Funding

S.D. was awarded a Doctoral Scholarship from the Natural Sciences and Engineering Research Council (NSERC) CREATE Program in Regenerative Medicine. C.R. was awarded an "AMX" Doctoral Scholarship from the Institut Polytechnique de Paris; The study was supported by the 'Fondation de l'Avenir' [RMA_2013]; the French National Research Agency (ANR) Project IMPLANTS [ANR-14-CE17-0014]; The MSDAVENIR (Meck Sharp and Dome AVENIR) program, project SAVE-BRAIN; and the Foundation for Medical Research (FRM) Programme 'Bioingénierie pour la Santé – 2014' [DBS20140930764]. The research program was also supported by the Institut National de la Santé et de la Recherche Médicale (INSERM); the 'Université de Paris'; the NSERC (Strategic Project); the Québec Ministry of Economy and Innovation (PSR Project); and the Quebec Ministry of International Relations.

Conflict of interest: none declared.

References

- Kornowski R, Hong MK, Virmani R, Jones R, Vodovotz Y, Leon MB. Granulomatous 'foreign body reactions' contribute to exaggerated in-stent restenosis. *Coron Artery Dis* 1999;**10**:9–14.
- Farb A, Sangiorgi G, Carter AJ, Walley VM, Edwards WD, Schwartz RS, Virmani R. Pathology of acute and chronic coronary stenting in humans. *Circulation* 1999;**99**:44–52.
- Morice MC, Serruys PW, Sousa JE, Fajadet J, Ban Hayashi E, Perin M, Colombo A, Schuler G, Barragan P, Guagliumi G, Molnar F, Falotico R. A randomized comparison of a sirolimus-eluting stent with a standard stent for coronary revascularization. *N Engl J Med* 2002;**346**:1773–1780.
- Solinas E, Dangas G, Kirtane AJ, Lansky AJ, Franklin-Bond T, Boland P, Syros G, Kim YH, Gupta A, Mintz G, Fahy M, Collins M, Kodali S, Stone GW, Moses JW, Leon MB, Mehran R. Angiographic patterns of drug-eluting stent restenosis and one-year outcomes after treatment with repeated percutaneous coronary intervention. *Am J Cardiol* 2008;**102**:311–315.
- Byrne RA, Iijima R, Mehilli J, Piniack S, Bruskina O, Schomig A, Kastrati A. Durability of antirestenotic efficacy in drug-eluting stents with and without permanent polymer. *JACC Cardiovasc Interv* 2009;**2**:291–299.
- Granada JF, Kaluza GL, Raizner A. Drug-eluting stents for cardiovascular disorders. *Curr Atheroscler Rep* 2003;**5**:308–316.
- Inoue T, Croce K, Morooka T, Sakuma M, Node K, Simon DI. Vascular inflammation and repair: implications for re-endothelialization, restenosis, and stent thrombosis. *JACC Cardiovasc Interv* 2011;**4**:1057–1066.
- Caligiuri G. Mechanotransduction, immunoregulation, and metabolic functions of CD31 in cardiovascular pathophysiology. *Cardiovasc Res* 2019;**115**:1425–1434.
- Caligiuri G. CD31 as a therapeutic target in atherosclerosis. *Circ Res* 2020;**126**:1178–1189.
- Diaz-Rodriguez S, Loy C, Chevallier P, Noel C, Caligiuri G, Houssiau L, Mantovani D. Comparison of the linking arm effect on the biological performance of a CD31 agonist directly grafted on L605 CoCr alloy by a plasma-based multistep strategy. *Biointerphases* 2019;**14**:051009.
- Andreatta F, Syvannarath V, Clement M, Delbosc S, Guedj K, Fornasa G, Khallou-Laschet J, Morvan M, Even G, Procopio E, Gaston AT, Le Borgne M, Deschamps L, Nicoletti A, Caligiuri G. Macrophage CD31 signaling in dissecting aortic aneurysm. *J Am Coll Cardiol* 2018;**72**:45–57.
- Batul R, Tamanna T, Khaliq A, Yu A. Recent progress in the biomedical applications of polydopamine nanostructures. *Biomater Sci* 2017;**5**:1204–1229.
- Luo R, Tang L, Wang J, Zhao Y, Tu Q, Weng Y, Shen R, Huang N. Improved immobilization of biomolecules to quinone-rich polydopamine for efficient surface functionalization. *Colloids Surf B Biointerfaces* 2013;**106**:66–73.

14. Dommerholt J, Schmidt S, Temming R, Hendriks LJ, Rutjes FP, van Hest JC, Lefeber DJ, Friedl P, van Delft FL. Readily accessible bicyclononynes for bioorthogonal labeling and three-dimensional imaging of living cells. *Angew Chem Int Ed Engl* 2010;**49**:9422–9425.
15. Levesque J, Hermawan H, Dube D, Mantovani D. Design of a pseudo-physiological test bench specific to the development of biodegradable metallic biomaterials. *Acta Biomater* 2008;**4**:284–295.
16. De Prado AP, Pérez-Martínez C, Cuellas-Ramón C, Gonzalo-Orden JM, Regueiro-Purriños M, Martínez B, García-Iglesias MJ, Ajenjo JM, Altónaga JR, Diego-Nieto A, De Miguel A, Fernández-Vázquez F. Time course of reendothelialization of stents in a normal coronary swine model. *Veterinary Pathology* 2011;**48**:1109–1117.
17. Wegner KA, Keikhosravi A, Eliceiri KW, Vezina CM. Fluorescence of picosirius red multiplexed with immunohistochemistry for the quantitative assessment of collagen in tissue sections. *J Histochem Cytochem* 2017;**65**:479–490.
18. Torii S, Jinnouchi H, Sakamoto A, Kutyna M, Cornelissen A, Kuntz S, Guo L, Mori H, Harari E, Paek KH, Fernandez R, Chahal D, Romero ME, Kolodgie FD, Gupta A, Virmani R, Finn AV. Drug-eluting coronary stents: insights from preclinical and pathology studies. *Nat Rev Cardiol* 2020;**17**:37–51.
19. Bridges AW, García AJ. Anti-inflammatory polymeric coatings for implantable biomaterials and devices. *J Diabetes Sci Technol* 2008;**2**:984–994.
20. Hauser D, Septiadi D, Turner J, Petri-Fink A, Rothen-Rutishauser B. From bioinspired glue to medicine: polydopamine as a biomedical material. *Materials* 2020;**13**:1730.
21. Duckers HJ, Soullie T, den Heijer P, Rensing B, de Winter RJ, Rau M, Mudra H, Silber S, Benit E, Verheye S, Wijns W, Serruys PW. Accelerated vascular repair following percutaneous coronary intervention by capture of endothelial progenitor cells promotes regression of neointimal growth at long term follow-up: final results of the Healing II trial using an endothelial progenitor cell capturing stent (Genous R stent). *EuroIntervention* 2007;**3**:350–358.
22. Giurgea GA, Heuberger A, Babayev J, Winkler S, Schlager O, Lang IM, Gyongyosi M. 9-year clinical follow-up of patients with ST-segment elevation myocardial infarction with Genous or TAXUS Liberté stents. *PLoS One* 2018;**13**:e0201416.
23. Klomp M, Beijik MA, Varma C, Koolen JJ, Teiger E, Richardt G, Bea F, van Geloven N, Verouden NJ, Chan YK, Woudstra P, Damman P, Tijssen JG, de Winter RJ. 1-Year outcome of TRIAS HR (TRI-stent adjudication study-high risk of restenosis) a multicenter, randomized trial comparing genous endothelial progenitor cell capturing stents with drug-eluting stents. *JACC Cardiovasc Interv* 2011;**4**:896–904.
24. den Dekker WK, Houtgraaf JH, Onuma Y, Benit E, de Winter RJ, Wijns W, Grisold M, Verheye S, Silber S, Teiger E, Rowland SM, Ligtenberg E, Hill J, Wiemer M, den Heijer P, Rensing BJ, Channon KM, Serruys PW, Duckers HJ. Final results of the HEALING IIB trial to evaluate a bio-engineered CD34 antibody coated stent (GenousStent) designed to promote vascular healing by capture of circulating endothelial progenitor cells in CAD patients. *Atherosclerosis* 2011;**219**:245–252.
25. Haude M, Lee SW, Worthley SG, Silber S, Verheye S, Erbs S, Rosli MA, Botelho R, Meredith I, Sim KH, Stella PR, Tan HC, Whitbourn R, Thambar S, Abizaid A, Koh TH, Den Heijer P, Parise H, Cristea E, Maehara A, Mehran R. The REMEDEE trial: a randomized comparison of a combination sirolimus-eluting endothelial progenitor cell capture stent with a paclitaxel-eluting stent. *JACC Cardiovasc Interv* 2013;**6**:334–343.
26. Saito S, Krucoff MW, Nakamura S, Mehran R, Maehara A, Al-Khalidi HR, Rowland SM, Tasissa G, Morrell D, Joseph D, Okaniwa Y, Shibata Y, Bertolet BD, Rothenberg MD, Genereux P, Bezerra H, Kong DF. Japan-United States of America Harmonized Assessment by Randomized Multicentre Study of OrbusNEich's Combo StEnt (Japan-USA HARMONEE) study: primary results of the pivotal registration study of combined endothelial progenitor cell capture and drug-eluting stent in patients with ischaemic coronary disease and non-ST-elevation acute coronary syndrome. *Eur Heart J* 2018;**39**:2460–2468.
27. Jaguszewski M, Aloysius R, Wang W, Bezerra HG, Hill J, De Winter RJ, Karjalainen PP, Verheye S, Wijns W, Luscher TF, Joner M, Costa M, Landmesser U. The REMEDEE-OCT study: an evaluation of the bioengineered COMBO dual-therapy CD34 antibody-covered sirolimus-eluting coronary stent compared with a Cobalt-Chromium everolimus-eluting stent in patients with acute coronary syndromes: insights from optical coherence tomography imaging analysis. *JACC Cardiovasc Interv* 2017;**10**:489–499.
28. Vasa M, Fichtlscherer S, Aicher A, Adler K, Urbich C, Martin H, Zeiher AM, Dimmeler S. Number and migratory activity of circulating endothelial progenitor cells inversely correlate with risk factors for coronary artery disease. *Circ Res* 2001;**89**:E1–7.
29. Blindt R, Vogt F, Astafieva I, Fach C, Hristov M, Krott N, Seitz B, Kapurniotu A, Kwok C, Dewor M, Bosserhoff AK, Bernhagen J, Hanrath P, Hoffmann R, Weber C. A novel drug-eluting stent coated with an integrin-binding cyclic Arg-Gly-Asp peptide inhibits neointimal hyperplasia by recruiting endothelial progenitor cells. *J Am Coll Cardiol* 2006;**47**:1786–1795.
30. Ruoslahti E. RGD and other recognition sequences for integrins. *Annu Rev Cell Dev Biol* 1996;**12**:697–715.
31. Bacakova L, Filova E, Kubies D, Machova L, Proks V, Malinova V, Lisa V, Rypacek F. Adhesion and growth of vascular smooth muscle cells in cultures on bioactive RGD peptide-carrying polylactides. *J Mater Sci Mater Med* 2007;**18**:1317–1323.